ARL-TR-9155 • MAR 2021

DEVCOM ARMY RESEARCH LABORATORY

Predicting M4 Carbine Pollutant Emissions: Baseline Skeletal Finite-Rate Chemical Kinetics Mechanisms for Muzzle-Blast Modeling

by Michael J McQuaid, Chiung-Chu Chen, Kevin L McNesby, and John R Schmidt

NOTICES

Disclaimers

The findings in this report are not to be construed as an official Department of the Army position unless so designated by other authorized documents.

Citation of manufacturer's or trade names does not constitute an official endorsement or approval of the use thereof.

Destroy this report when it is no longer needed. Do not return it to the originator.

ARL-TR-9155 ● MAR 2021

Predicting M4 Carbine Pollutant Emissions: Baseline Skeletal Finite-Rate Chemical Kinetics Mechanisms for Muzzle-Blast Modeling

Michael J McQuaid, Chiung-Chu Chen, Kevin L McNesby, and John R Schmidt
Weapons and Materials Research Directorate,
DEVCOM Army Research Laboratory

REPORT DOCUMENTATION PAGE

Form Approved
OMB No. 0704-0188

1. REPORT DATE *(DD-MM-YYYY)*	2. REPORT TYPE	3. DATES COVERED (From - To)
March 2021	Technical Report	1 October 2020–31 January 2021

4. TITLE AND SUBTITLE
Predicting M4 Carbine Pollutant Emissions: Baseline Skeletal Finite-Rate Chemical Kinetics Mechanisms for Muzzle-Blast Modeling

5a. CONTRACT NUMBER

5b. GRANT NUMBER

5c. PROGRAM ELEMENT NUMBER

6. AUTHOR(S)
Michael J McQuaid, Chiung-Chu Chen, Kevin L McNesby, and John R Schmidt

5d. PROJECT NUMBER
WP19-1392

5e. TASK NUMBER

5f. WORK UNIT NUMBER

7. PERFORMING ORGANIZATION NAME(S) AND ADDRESS(ES)
DEVCOM Army Research Laboratory
ATTN: FCDD-RLW-WC
Aberdeen Proving Ground, MD 21005-5067

8. PERFORMING ORGANIZATION REPORT NUMBER
ARL-TR-9155

9. SPONSORING/MONITORING AGENCY NAME(S) AND ADDRESS(ES)
Strategic Environmental Research and Development Program
4800 Mark Center Drive, Suite 16F16
Alexandria, VA 22350-3605

10. SPONSOR/MONITOR'S ACRONYM(S)
SERDP

11. SPONSOR/MONITOR'S REPORT NUMBER(S)

12. DISTRIBUTION/AVAILABILITY STATEMENT
Approved for public release: distribution unlimited.

13. SUPPLEMENTARY NOTES
ORCID IDs: Michael J McQuaid, 0000-00015523-7468; Chiung-Chu Chen, 0000-0002-8666-9949

14. ABSTRACT
To create baseline chemical kinetics mechanisms for a computational fluid dynamics (CFD) model of M4 muzzle blast, the trial mechanism method was employed to reduce a "full" mechanism comprising 2751 elementary reactions and 813 species. The full mechanism's appropriateness for the application is discussed. Solutions to relevant homogeneous reactor problems based on skeletal mechanisms with as few as 22 reactions and 20 species yielded temperature and heat release rate versus time histories that well reproduced those produced with the full mechanism. Two candidates were recommended for use in the muzzle-blast CFD model: one with 22 reactions and 20 species, and one with 27 reactions and 22 species. All the inputs needed to construct them are provided in an addendum to this report (ARL-TN-1048). Targeting the establishment of better-designed screening protocols for future mechanism reduction efforts, recommendations for mapping the results of muzzle-blast simulations produced with these mechanisms are proffered.

15. SUBJECT TERMS
muzzle blast, pollutant emissions, M4 carbine, chemical kinetics, computational fluid dynamics

16. SECURITY CLASSIFICATION OF:			17. LIMITATION OF ABSTRACT	18. NUMBER OF PAGES	19a. NAME OF RESPONSIBLE PERSON
a. REPORT	b. ABSTRACT	c. THIS PAGE			Michael J McQuaid
Unclassified	Unclassified	Unclassified	UU	34	19b. TELEPHONE NUMBER (Include area code) (410) 278-6185

Contents

List of Figures

List of Tables

Acknowledgments

This effort was sponsored by the Strategic Environmental Research and Development Program (Project WP19-1392). The screening protocols were performed on a Department of Defense Shared Resource Center High Performance Computing platform at the US Army Combat Capabilities Development Command Army Research Laboratory, Aberdeen Proving Ground, Maryland.

1. Introduction

Sponsored by the Strategic Environmental Research and Development Program (Project WP19-1392), US Army Combat Capabilities Development Command Army Research Laboratory and US Environmental Protection Agency researchers are developing methodologies that will improve the measurement and prediction of armament pollutant emissions produced by the combustion of metal-containing propellants, pyrotechnics, and explosives. Among the armaments for which better emission predictions are sought is the M4 carbine (McNesby et al. 2018). The M4 is the standard service rifle issued to most US military combat units. It fires M855 (5.56- × 45-mm NATO) cartridges, and the propelling charge in these cartridges is a ball powder formulated with nitrocellulose (NC) and nitroglycerine (NG).

The modeling approach for predicting pollutant emission levels produced by combustion of the ball powder during M4 firings was formulated based on DEVCOM Army Research Laboratory's experience in developing and applying computational fluid dynamics (CFD) models for simulating the interior ballistic (IB) cycles of gun and rocket propulsion systems. Briefly, the products of the ball powder's combustion during the IB cycle are to be predicted as they are in current state-of-the-art gun IB models, and the continuation of the process in the atmosphere is to be predicted as it is in current state-of-the-art rocket IB models. In both cases, the processes are formulated in terms of the Navier–Stokes (NS) equations for mass, momentum, and energy transport. The primary difference between them is the manner in which the gas phase's chemical kinetics are handled. In the former, they are assumed to go "instantaneously" to completion (i.e., an equilibrium state), and relevant properties of the "working fluid"/gas are derived on the basis of thermochemical equilibrium calculations (Horst 2005; Mayer and Hart 1945). In the latter, they are represented with a detailed finite-rate mechanism. The difference, which is based on the difference in the temperature (T) and pressure (P) ranges relevant to gun and rocket motor IB cycles, impacts both the reliability of a CFD model's predictions and its computational cost. Both increase with the inclusion of a finite-rate mechanism, the latter significantly.

Given that the products of the ball powder's combustion transition through T and P ranges similar to those of typical rocket-motor IB cycles, we believed that a finite-rate mechanism would be needed to obtain reliable pollutant emission level predictions. However, we also expected that it would be computationally infeasible to model the process from ignition to its conclusion on that basis. That expectation was based on the following considerations.

A detailed finite-rate chemical kinetics mechanism is a network comprising molecular and/or atomic species (k) connected by elementary reactions (i). For each reaction, it specifies parameters for calculating rates of species conversion (R_i) via the law of mass action (Benson 1976). To enforce species conservation, NS-based CFD models that include a detailed mechanism must add to the (five) partial differential equations (PDEs) needed to enforce mass, momentum, and energy conservation, a PDE for each species in the mechanism. In addition, each reaction adds a source term to each PDE. Therefore, the incorporation of a detailed mechanism into a CFD model engenders a computational cost that scales with the numbers of reactions and species in the mechanism, and the dependence is quadratic to cubic (Stone 2020).

Dependent also on the number of grid points needed to adequately discretize the model's spatial domain (which can run into the millions), and the number of time steps needed to resolve temporal transients (which can also run into the millions), computational costs limit the numbers of reactions and species that can be included in a mechanism. For CFD models of tactical rocket-motor combustors, current limits are approximately 120 reactions and 100 species. (For comparison, a comprehensive mechanism Chen et al. [2019] assembled for modeling the combustion of NG comprised 1075 reactions and 189 species.) Including both the interior volume of the M4's barrel and the volume into which the effluent expands after the bullet exits the barrel, the spatial domain/volume (V) relevant to an M4 firing is considerably larger than the domains of tactical rocket-motor combustors, making it possible that even-more-restrictive limits might have to be imposed.

Expecting the numbers of reactions and species that could be included in the finite-rate mechanism would be extremely limited, we anticipated the need to be judicious in their application. The proposed modeling approach was conceived with that in mind. Because R_i tend to increase with increases in T and/or P, and T and P are extremely high during the M4's IB cycle, it is reasonable to assume that the time scale of the gas-phase chemical kinetics associated with the ball powder's combustion is negligibly short compared to the time scale of the cycle. Therefore, chemical compositions ($\{X_k\}$) derived on the basis of thermochemical equilibrium calculations (where X_k is the mole fraction of the kth species) reasonably approximate those that are actually produced. The reliability of the results produced by current state-of-the-art gun IB models attest to that. Establishing a boundary condition for the subsequent expansion of the combustion products into the atmosphere, which is referred to herein as "muzzle blast", this paradigm reduces the (T, P, $\{X_k\}$) parameter space over which the chemical kinetics mechanism needs to be valid and therefore has the potential to reduce the mechanism's size. Indeed, for any X_k threshold set to establish whether a potential combustion product needs

be included in the chemical kinetics mechanism (regardless of its potential to react as the effluent from the muzzle expands and mixes with air), the number of species composing this state will be less than that of any state produced by advanced but incomplete combustion. As such, it establishes the baseline/minimum set that any mechanism that is to be a basis for predicting M4 pollutant emissions must include.

Our approach to developing and validating finite-rate mechanisms for muzzle-blast modeling was also based on our experience in developing them for rocket-motor IB models. Briefly, it entailed selecting a full/comprehensive mechanism deemed capable of well representing the chemical kinetics within the (T, P, $\{X_k\}$) parameter space of interest and deriving from it skeletal mechanisms able to reasonably mimic the full one within that space.

For the full mechanism, we selected a mechanism we had previously assembled to model the combustion of hydroxyl-terminated polybutadiene (HTPB) (Chen and McQuaid 2009, 2010, 2011, 2015, 2020). Comprising 2751 elementary reactions and 813 (atomic/molecular) species, this mechanism was built in several stages. The first stage targeted the establishment of a basis for modeling the chemical kinetics in a hybrid rocket-motor combustor in which HTPB was the primary component of the fuel grain and red fuming nitric acid (RFNA) was the oxidizer (Chen and McQuaid 2009, 2010). Reactions and species were added to that construct to establish a basis for modeling HTPB–air combustion (Chen and McQuaid 2011). That version was further updated and modified in the course of developing mechanisms for modeling the combustion of other HTPB-containing rocket propellants (Chen and McQuaid 2015, 2020). Although the chemical kinetics driving the IB cycles of the propulsion system concepts for which this mechanism was developed are far removed from the one of interest, the ($C_wH_xN_yO_z$) end products of HTPB–RFNA combustion are the same as those generated by the complete combustion of typical NC–NG-based ball powders, and that knowledge informed the development of the initial construct. In short, a mechanism Anderson et al. (2011a, b) had assembled to model the "dark zones" observed in the combustion of nitrate-ester-based energetic materials was included in toto.

The reason we planned to reduce the full HTPB–RFNA–air mechanism rather than the HTPB–RFNA mechanism (or Anderson et al.'s dark-zone mechanism for that matter) is that oxygen (O_2) does not generally play an important role during either a gun IB cycle or an HTPB–RFNA-fueled hybrid motor firing. Fully expecting that it would in muzzle blast, we were concerned that the HTPB–RFNA mechanism alone would not provide a sufficiently comprehensive basis for modeling it. We had no such qualms about the full HTPB–RFNA–air mechanism. Indeed, containing reactions for the decomposition (and production) of molecules with up

to 20 carbon (C) atoms, the network composing it was deemed likely to be far more extensive than needed for establishing a "baseline"/minimal mechanism for modeling muzzle-blast chemical kinetics. Based on previous experience, we knew that if the combustion of the ball powder was assumed to be complete at the end of the IB cycle, the X_k of species containing more than one or two C atoms would be negligible. Moreover, we knew that though the temperature of the effluent from the muzzle would in the main decrease as it expanded into the atmosphere, and therefore have the potential to produce larger species, that potential would be small. Nevertheless, we wanted a mechanism with the potential to produce larger species if the process had more potential for that than expected. Moreover, the full HTPB–RFNA–air mechanism has the potential to be a basis for developing mechanisms for predicting the fate of moieties present due to incomplete combustion.

The generation of skeletal mechanisms from the full HTPB–RFNA–air mechanism was accomplished via the trial mechanism method (TMM). The TMM (concept) predicates the elimination of reactions from a full/comprehensive mechanism based on comparisons of full- and trial-mechanism-based solutions to combustion problems that are relevant to, but (significantly) less expensive to solve than, those of specific interest. This report summarizes the factors considered in formulating a screening protocol to create skeletal mechanisms for muzzle-blast modeling. Briefly, a series of thermochemical equilibrium calculations was performed to estimate the T, P, and $\{X_k\}$ of the gas in an M4's barrel at the end of the IB cycle. Translated into initial conditions for homogeneous reactor (HR) simulations conceived to involve chemical kinetics relevant to muzzle blast, they were modified to include an amount of air that might be expected to mix with the effluent during the first millisecond following the bullet's exit from the muzzle. Observing that heat was generated upon the mixture's (closed, adiabatic) expansion, we employed an adiabatic constant pressure (CONP) problem as the basis for the protocol. It was found that solutions based on skeletal mechanisms with as few 22 reactions and 20 species yielded T and heat release rate ($\dot{q}$) versus time (t) histories that reasonably reproduced those produced with the full mechanism. Subsequently employed as bases for solving a programmed V expansion versus t (VTIM) problem that was considered a better approximation of an actual blast, those mechanisms also produced solutions that yielded T and $\dot{q}$ versus t histories that were in good agreement with those produced with the full mechanism. Comparisons are presented and discussed.

Two candidates were recommended for use in the muzzle-blast CFD model. All the inputs needed to construct them are provided in an addendum to this report (McQuaid et al. 2021). For convenience, parameter sets for computing the species'

molecular transport properties are also provided in the addendum. Toward establishing better-designed screening protocols for future mechanism-reduction efforts, recommendations for mapping the results of muzzle-blast simulations produced with these mechanisms are proffered.

2. Trial Mechanism Method

More-complete descriptions of the TMM are given elsewhere (Kotlar 2010; McQuaid 2013a). Basic screening protocol steps include the following:

- Randomly ordering the starting mechanism's reactions
- Sequentially eliminating (single) reactions from it on a trial basis
- For each elimination, solving a canonical combustion problem (or problems) with the trial mechanism created by the elimination
- Permanently eliminating a reaction if changes in the values of selected parameters of the solution(s) do not exceed specified criteria

A species is eliminated as a consequence of all reactions involving it being eliminated. Specifics of the screening protocol employed for the current effort were as follows.

2.1 Canonical Combustion Problem Selection

While there are many combustion problem types that could be imagined as being bases for a TMM screening protocol, there have only been two that have been employed by our group: 1) closed-system, adiabatic HR problems (as prescribed by SENKIN [Lutz et al. 1988]), and 2) 1-D steady laminar opposed-flow diffusion flame (OFDF) problems (as prescribed by OPPDIF [Lutz et al. 1997]). Because HR problems are considerably less demanding to formulate and solve than OFDF problems, they were employed for the original development and application of the TMM (Kotlar 2010; McQuaid 2013a). Indeed, until the past year, there had been no compelling reason to formulate screening protocols based on OFDF problems. In short, for all applications for which HR-based screening protocols were developed and applied, skeletal mechanisms with targeted sizes were produced, and evidence suggesting they were producing poor results in the applications of interest was not observed.

That history notwithstanding, muzzle blast involves the expansion of a relatively high-density "fuel" into a low-pressure oxidizer, and (by definition) all species in an HR simulation are fully mixed at all times. (As is discussed later in this report, the density of the gas in the barrel is approximately one-fifth the density of liquid

water, so we imagine that the muzzle-blast flow field is akin to water issuing from a hose into ambient air. Various published studies support this conception [Zhang et al. 2013].) Since it cannot be expected that the chemical kinetics in a dominantly nonpremixed flow field will be mirrored in an HR simulation, the potential for an HR-based screening protocol to produce skeletal mechanisms that will mimic well a full one's capacity to represent muzzle-blast chemical kinetics was/is somewhat speculative. Moreover, molecular transport/diffusion may also be germane, but it does not play a role in HR simulations. As such, there could be reactions and species in the candidates produced on such bases that are unnecessary for modeling the dynamics of interest. In addition, there may be some reactions and species whose addition to the reduced mechanism would improve its capacity to mimic the full mechanism within the parameter space of interest.

Foreseeing that such concerns might not be able to be overlooked in the reduction of mechanisms for modeling reacting flows in a solid-fuel ramjet combustor, the first author of this report developed and tested an OFDF-based screening protocol for that application, and it appeared to have the potential to address those concerns (McQuaid 2020). However, we did not believe we had enough information about the muzzle-blast flow field to be confident in formulating an OFDF problem that would be representative of it. Resources would also have been a problem. An OFDF-based screening protocol is considerably more expensive to set up and perform than an HR-based screening protocol. Therefore, we settled for the latter.

With respect to the selection of an HR problem type to employ for the screening protocol, we thought that of the types coded for in our (customized) SENKIN suite, a VTIM problem would be the best approximation to muzzle blast. However, we found that a VTIM problem we had formulated for the screening protocol was not properly solved within the TMM program. After several attempts to resolve that issue failed, and uncertain as to how much more effort would be required, we decided to employ a CONP problem instead. Our expectation was that the chemical kinetics driving the two (simulated) processes would be similar and that we could verify that as part of the candidate evaluation process.

2.2 Homogenous Reactor Simulations

2.2.1 Initial Conditions

Several steps were involved in establishing the initial conditions for the CONP problem employed for the screening protocol as well as the VTIM problem employed to further evaluate candidates. Targeting the creation of a mechanism suitable for muzzle-blast CFD simulations in which complete combustion of the propelling charge will be assumed, Cheetah (Bastea 2019) gun calculations were

performed to obtain estimates for the (nominal) T, P, and $\{X_k\}$ of the gas in the barrel of an M4 at the moment the bullet exits the muzzle. The nominal C-H-N-O stoichiometry ($C_{6.0476}H_{7.5213}N_{2.5194}O_{8.8874}$) and enthalpy of formation (–536.1 cal/g) of the propelling charge were calculated on the basis of a formulation corresponding to SMP-843. The relationship between P, T, and density (ρ), was based on a virial equation of state. A Blake product library was employed as the basis for calculating the thermodynamic properties of potential products.

Because the P-T-ρ relationship in the HR models was based on the ideal gas law, and the thermodynamic property prescriptions for species in the HTPB–RFNA–air mechanism and the Blake library were (presumably) not identical, the equilibria (eq) predicted by the gun calculations (T_{eq}, P_{eq}, $\{X_{eq,k}\}$) did not correspond to equilibria in the HR models. To translate the former into the latter, a series of adiabatic constant volume simulations were performed. Starting with a $\{X_{eq,k}\}$ produced by one of the gun calculations, and excluding species for which $X_{eq,k} < 1 \times 10^{-6}$ (with O_2 being one of them), T_0 and P_0 were adjusted to obtain a ρ_0 that would correspond to the initial mass of the propelling charge (1.639 g) divided by the volume of the barrel (8.94 cm^3) (i.e., 0.183 g/cm^3). T_0, P_0, and $\{X_{0,k}\}$ were then iterated until the initial state (T_0, P_0, $\{X_{0,k}\}$) and the final state (T_f, P_f, $\{X_{f,k}\}$) were approximately the same. Of course, that could be achieved for a range of T_0–P_0 combinations. Based on Cheetah-computed T_{eq} and P_{eq} values, we targeted an initial state in which T_0 was approximately 1750 K and P_0 was approximately 1000 atm.

To create a system in which that state could react with air, we added to it a mass of air equal to that which would be found at ambient conditions (300 K, 1 atm) in a cylindrical volume with a diameter equal to that of the bullet (5.56 mm) and a length equal to the distance between the breech and the leading edge of the effluent 1 ms after the bullet exits the muzzle. Based on the measurement-based data shown in Fig. 1, that volume was approximately 18 cm^3 (making it approximately twice the volume of the M4's barrel). Though somewhat arbitrary, that selection was based on envisioning the air in the bullet's path streaming back over the bullet and reacting with the fuel-rich effluent expanding behind it. Having been compressed, and therefore having a higher temperature and pressure than the ambient air, its addition to the propellant's combustion products at T_0 and P_0 could be rationalized (to a degree). (Discussed later in this report, simulations based on the mechanisms selected for incorporation into the muzzle-blast CFD model can be analyzed to evaluate this conjecture.) Based on the ideal gas law, such a volume would contain 3.66×10^{-4} moles of "air". Further specified to comprise 78 mol% nitrogen (N_2), 21 mol% oxygen (O_2), and 1 mol% argon (Ar), its effective molecular weight was 29.0 g/mol and its mass 0.02 g. Added to the mass of the propellant combustion

products, that value increased the system's initial ρ_0 to 0.185 g/cm^3. That value could have been produced by increasing P_0 and/or decreasing T_0. However, since the $\{X_{eq,k}\}$ values that were the basis for the combustion products' $\{X_{0,k}\}$ were more sensitive to changes in T than P, we simply increased P_0 to obtain the desired ρ_0.

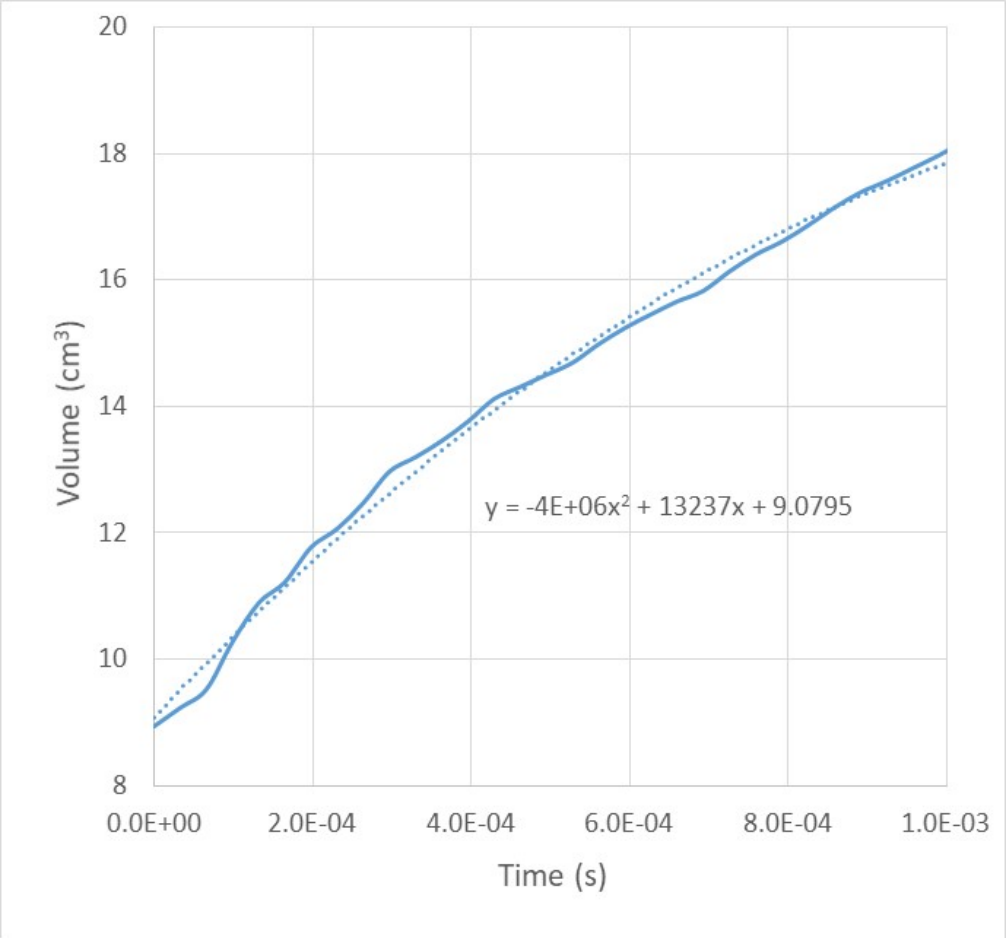

Fig. 1 Volume of a 5.56-mm-diameter cylinder extending from the breech to the leading edge of the effluent as a function of time following the bullet's exit from the muzzle

The initial conditions established on that basis are shown in Table 1. The starting chemical composition comprised 14 species, 12 of which were propellant combustion products. The sum of the $X_{0,k}$ for just five of them—carbon monoxide (CO), water (H_2O), carbon dioxide (CO_2), N_2, and hydrogen (H_2)—was greater than 0.99. The value of $X_{0,O2}$ (0.00235 or 0.235%) was due solely to the addition of air to the mixture. Extremely small compared with those of the major combustion products that could potentially be further oxidized, namely H_2 and CO, it comported with our sense for what O_2's concentration would be in regions of the flow field where the temperature would be high enough for it react at a non-negligible rate during the time scale of interest.

Table 1 Initial conditions for HR simulations

Parameter	Unit(s)	Value
T_0	K	1750.0
P_0	atm	1041.6
ρ_0	g/cm^3	0.18532
X_0	mol/mol	…
CO		0.360641
H_2O		0.200049
CO_2		0.173152
N_2		0.138063
H_2		0.124202
O_2		0.002347
CH_4		0.000929
NH_3		0.000402
Ar		0.000112
HCN		0.000044
HOCHO		0.000025
HNCO		0.000023
CH_2O		0.000011
H		0.000002

To simulate (to a degree) the muzzle-blast expansion process, we formulated VTIM problems in which the effluent's initial volume (V_0) equaled the interior volume of the M4's barrel and subsequently expanded at a programmed rate [$dV(t)/dt$]. The specification of $V(t)$ was (partially) informed by Edgerton shadowgraphs of M4 muzzle blast that provided measurements of the distance between the end of the barrel and the effluent's leading edge as a function of t (McNesby et al. 2018). Two extremes for the expansion rate were hypothesized: 1) a maximum corresponding to a spherical volume with a diameter equal to the distance between the end of the barrel and the effluent's leading edge, and 2) a minimum corresponding to the volume enclosed by a cylinder with a (fixed) diameter equal to the diameter of the bullet and an axial length equal to the distance between the breech and the effluent's leading edge. (The latter is a minimum because the effluent also expands in the radial direction.)

We found that the solution to the VTIM problem formulated on the basis of the maximum hypothesized expansion rate evolved to unrealistically low pressures and temperatures within the time scale of the measurements. Therefore, no further consideration was given to that problem.

The $V(t)$ corresponding to the minimum hypothesized expansion rate is shown in Fig. 1. For computational convenience, the second-order polynomial fit to the measurement-based values shown in the figure was used to calculate $V(t)$ and

$dV(t)/dt$ at a given t. The solution to the VTIM problem formulated on that basis did not raise any particular concern. Indeed, although $V(t)$ values calculated on that basis would be less than those encompassing the bulk of the effluent from the M4's barrel, we did not believe that trying to put too fine a point on them was warranted at this stage of the project. As is discussed later in this report, the largest changes in chemical composition that occurred in the HR simulations took place within the first microsecond, and we did not believe that a (reasonable) increase in the expansion rate would change that finding or significantly promote the formation of larger species. Therefore, we believed refinements should await the production and analysis of muzzle-blast CFD simulations.

2.2.2 Screened Parameters

As in prior TMM-based reductions performed by Kotlar (2010) and McQuaid and coworkers (McQuaid 2013a; Chen and McQuaid 2016, 2020; McQuaid et al. 2019), the parameters of the solution to the CONP problem whose values were compared were local maxima in the mass-specific and volumetric heat-release rates ($\dot{q}_m^{max}$ and $\dot{q}_v^{max}$, respectively) versus t histories, the times at which those maxima occurred (t_m^{max} and t_v^{max}, respectively), and the temperature at the end of the simulation (T_f). The rationale for comparing the values of these (and only these) parameters has been discussed previously (McQuaid 2013b). The values of $\dot{q}_m$ and $\dot{q}_v$ at a given t were calculated per

$$\dot{q}_m = R\left(T\sum_k^K \frac{dY_k}{dt}/W_k + \frac{dT}{dt}\sum_k^K Y_k/W_k\right) \quad (1)$$

and

$$\dot{q}_v = \rho * \dot{q}_m, \quad (2)$$

respectively, where R is the universal gas constant, and for a mechanism with K species, Y_k is the mass fraction of the k^{th} species and W_k is its molecular weight.

2.2.3 Convergence Criteria and Initial Screening

The subroutines employed to formulate the HR problems were derived from precommercial CHEMKIN subroutine libraries (Kee et al. 2002). The problems' differential-algebraic equation systems were solved with DASPK (Li and Petzold 1999). Stone (2020) refactored a number of subroutines in the two libraries, enabling them to exploit OpenMP parallelism and thereby reduce simulation run times.

To determine if a solution is "converged", DASPK calculates a weighted root-mean-square norm based on two user-specified parameters: a relative

tolerance (RTOL) and an absolute tolerance (ATOL). Reflecting the accuracy in a solution's state variables, their values can impact DASPK's ability to produce a converged solution and the calculation's runtime. (Decreasing their values tends to make convergence more difficult to achieve and increase runtimes.) However, it is not generally obvious what their values need to be to yield "desired accuracies" in T and $\dot{q}$, or how they might be established in an a priori manner. Therefore, given the negative ramifications of specifying overly small RTOL and ATOL values, we compared T and $\dot{q}$ versus t histories produced with values that spanned several orders of magnitude to find values below which "noticeable" changes stopped. It was found that runtimes were manageable with RTOL = 1×10^{-7} and ATOL = 1×10^{-12}, and that those specifications were well below the thresholds above which changes to T and $\dot{q}$ versus t histories became noticeable.

In addition, we assumed that, like the value of the analogous parameter in DASAC (Caracotsios and Stewart 1985), ATOL's value was "less than the smallest meaningful value of the species mass fraction" (Lutz et al. 1988). Therefore, we evaluated its use as a basis for the first step of the reduction. In short, all species (and all reactions involving them) whose mass fraction did not exceed 1×10^{-13} at any point during the simulation were eliminated. Not surprisingly (given our suspicion that much of the network prescribed by the full HTPB–RFNA–air mechanism would be superfluous with respect to creating a baseline mechanism for muzzle-blast modeling), large numbers of species and reactions were eliminated on this basis alone. Only 914 reactions and 132 species remained. Observing that the T and $\dot{q}$ versus t histories produced with this mechanism were indistinguishable from those produced with the full mechanism (at the scales at which they were plotted), we employed that subset as the starting point for further reduction.

3. Results

3.1 Candidate Generation

A total of 120 different orderings of the 914-reaction, 132-species mechanism's reactions were processed. They were submitted in two sets of 60. For the first set, the screening protocol specified maximum acceptable deviations (MADs) in $\dot{q}_m^{max}$, $\dot{q}_v^{max}$, t_m^{max}, t_v^{max}, and T_f that were similar to those employed for previous reduction efforts (e.g., Chen and McQuaid 2020). The initial MADs in $\dot{q}_m^{max}$, $\dot{q}_v^{max}$, t_m^{max}, and t_v^{max} were set at ±0.5%, and the MAD in T_f was set at ±0.5 K. Those values were subsequently (and collectively) relaxed in ±0.5% and ±0.5-K increments, respectively, and the maximum MADs allowed were ±10% and ±10 K. That protocol produced candidates with as few as 19 reactions and 14 species, and

all orderings produced candidates with 20 or fewer reactions and 17 or fewer species.

Given that the number of species in the smallest candidate produced by the first protocol equaled the number of species present at t_0, a muzzle-blast CFD model employing it would not have the potential to create new species. Desiring that potential and believing that the incorporation of larger mechanisms into the CFD model would be feasible, we processed the second set of orderings via a protocol in which the initial MADs in $\dot{q}_m^{max}$, $\dot{q}_v^{max}$, t_m^{max}, and t_v^{max} were set at ±0.1%, and the MAD in T_f was set at ±0.2 K. Those values were subsequently (and collectively) relaxed in ±0.1% and ±0.2-K increments, respectively. The maximum MADs in $\dot{q}_m^{max}$, $\dot{q}_v^{max}$, t_m^{max}, and t_v^{max} allowed were ±2.0%. The maximum MAD in T_f allowed was ±4.0 K.

All but 2 of the 60 orderings processed with the second protocol produced candidates with 32 or fewer reactions and 22 or fewer species. The smallest candidate comprised 22 reactions and 20 species, and it was selected for further evaluation. It is referred to hereafter as SM(22R-20S). A second candidate comprising 27 reactions and 22 species was also selected for further evaluation. Referred to hereafter as SM(27R-22S), it included all the reactions and species composing SM(22R-20S). All the inputs needed to construct these mechanisms are provided in an addendum to this report (McQuaid et al. 2021).

3.2 Post-Reduction Analyses

3.2.1 Screening Protocol Simulation

Figure 2 compares the T and $\dot{q}_m$ versus t histories obtained from full mechanism-, SM(22R-20S)-, and SM(27R-22S)-based solutions to the CONP problem that was the basis for the TMM's screening protocol. Reactions induced by the added O_2 produced only one significant heat-release event. It was effectively complete within 1 μs of the process's onset, and led to an increase in the temperature of about 27 K. As shown, the histories produced with SM(22R-20S) and SM(27R-22S) were in reasonable agreement with those produced with the full mechanism, confirming they were not "false positives".

T and $\dot{q}_m$ versus t histories produced with mechanisms having sizes intermediate to SM(22R-20S)'s and SM(27R-22S)'s were also plotted, but none were in as good agreement with those produced by the full mechanism as those produced with SM(27R-22S). In addition, because the histories produced with SM(27R-22S) were almost indistinguishable from those produced with the full mechanism, we did not evaluate any histories produced with larger mechanisms.

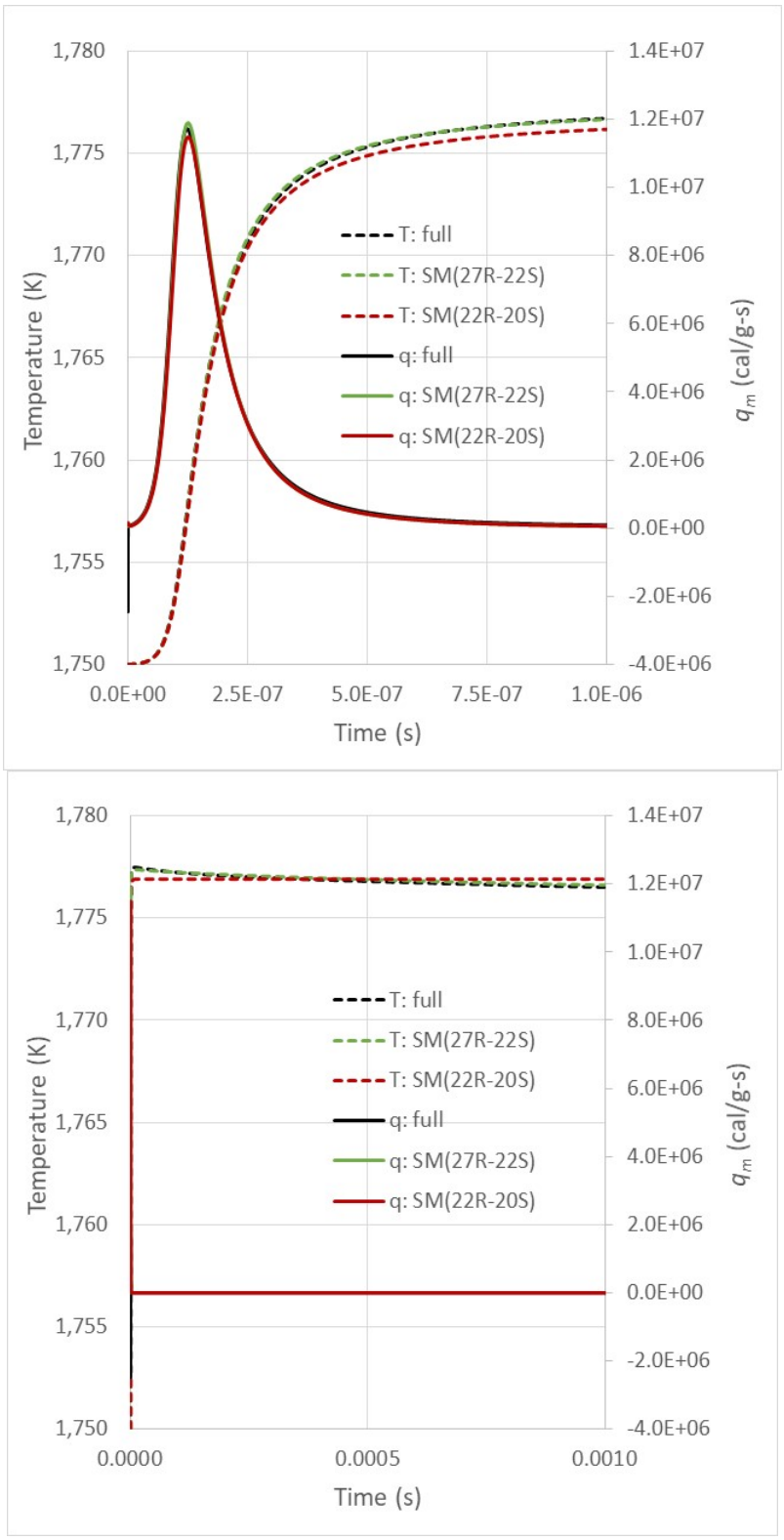

Fig. 2 ***T*** **and** $\dot{q}_m$ **vs.** ***t*** **histories obtained from full-mechanism-based and SM(22R-20S)- and SM(27R-22S)-based solutions to the screening protocol's CONP problem. Note the difference in time scales.**

3.2.2 Validation Simulation

Figure 3 compares the T and $\dot{q}_m$ versus t histories obtained from full-mechanism-based and SM(22R-20S)- and SM(27R-22S)-based solutions to the VTIM problem employed for validation purposes. As in the CONP simulation discussed in the previous section, reactions induced by the added O_2 produced a single significant heat-release event, and it was effectively complete within 1 μs of the process's onset. Somewhat surprisingly, the initial temperature rise was slightly larger than it was in the case of the CONP simulation: 32 versus 27 K, indicating the (programmed) expansion rate was somewhat slower during this time frame. However, the temperature fell below 1777 K within 10 μs, and a decrease in the temperature of over 200 K occurred within the first millisecond. Again, the histories produced with SM(22R-20S) agreed well with those produced by the full mechanism. The histories produced with SM(27R-22S) were almost indistinguishable from those produced with the full mechanism.

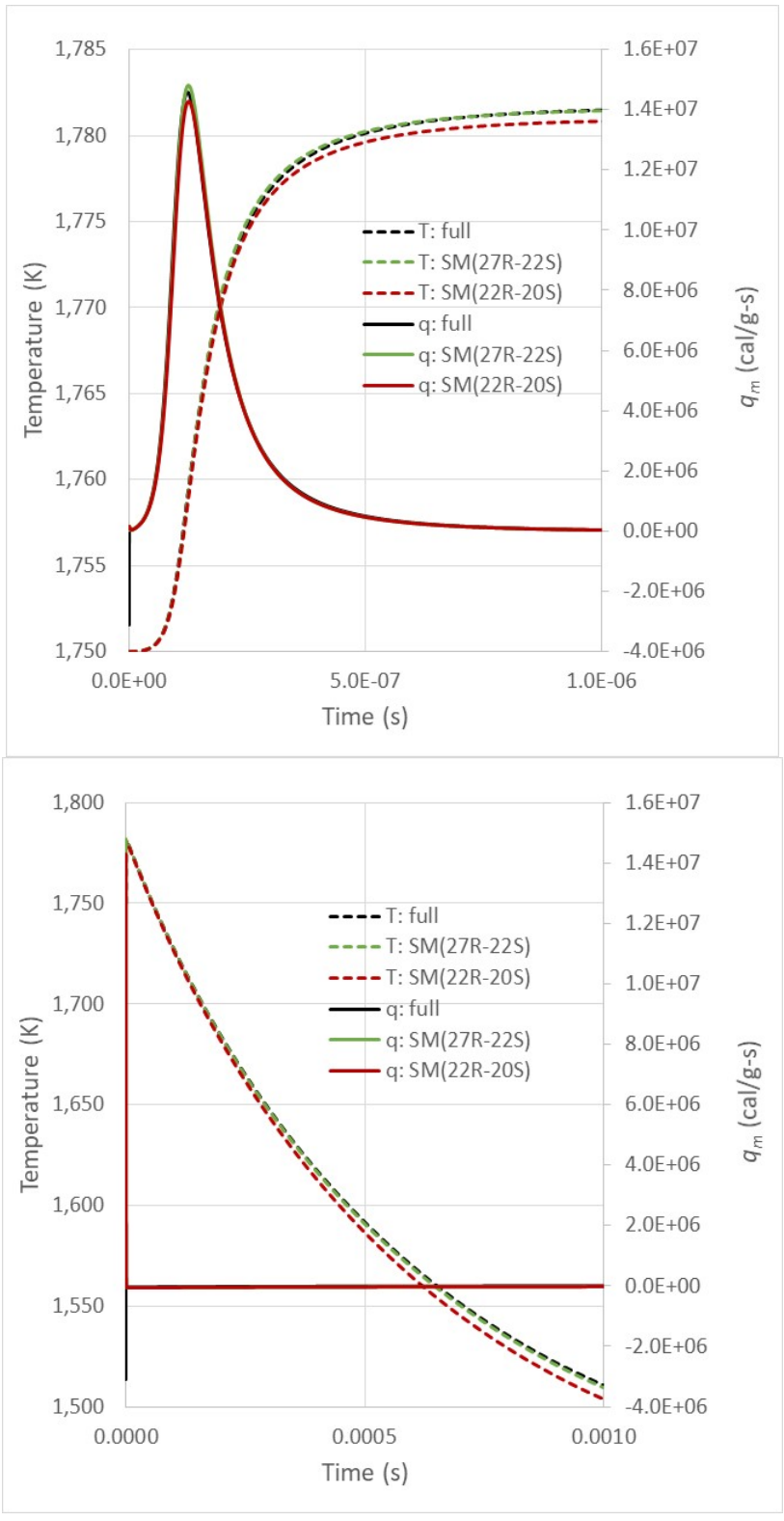

Fig. 3 T and $\dot{q}_m$ vs. t histories obtained from full-mechanism-based and SM(22R-20S)- and SM(27R-22S)-based solutions to a muzzle-blast-relevant VTIM problem. Note the difference in time scales.

3.2.3 Species Profiles

Table 2 lists the species composing the initial chemical composition of the HR simulations, SM(22R-20S), and SM(27R-22S). In the mechanisms' lists, a species is designated "reactive" if it is involved in at least one elementary reaction that creates and/or decomposes it. As detailed in the addendum to this report (McQuaid et al. 2021), 17 of the 22 reactions in SM(22R-20S) involve species in which the only elements are H and/or O. In addition, one of the species produced by that submechanism (HO_2) can react with CO to produce CO_2. These results suggest that any further oxidation of combustion products produced during the IB cycle will largely be mediated by radicals created via the O_2-enabled oxidation of H_2.

Table 2 Species present at t_0 in the HR simulations and those composing SM(22R-20S) and SM(27R-22S)

	Species	Present at t_0	SM(22R-20S)	SM(27R-22S)
1	CO	Yes	reactive	reactive
2	H_2O	Yes	reactive	reactive
3	CO_2	Yes	reactive	reactive
4	N_2	Yes	nonreactive	nonreactive
5	H_2	Yes	reactive	reactive
6	O_2	Yes	reactive	reactive
7	CH_4	Yes	reactive	reactive
8	NH_3	Yes	nonreactive	nonreactive
9	Ar	Yes	nonreactive	nonreactive
10	HCN	Yes	nonreactive	nonreactive
11	HOCHO	Yes	nonreactive	nonreactive
12	HNCO	Yes	nonreactive	nonreactive
13	CH_2O	Yes	nonreactive	reactive
14	H	Yes	reactive	reactive
15	HO_2	No	reactive	reactive
16	O	No	reactive	reactive
17	OH	No	reactive	reactive
18	CH_3	No	reactive	reactive
19	HCO	No	reactive	reactive
20	H_2O_2	No	reactive	reactive
21	CH_3O	No	…	reactive
22	CH_3OCO	No	…	reactive

No reactions involving N-atom-containing species were in either mechanism. In general, N_2 is not very reactive at temperatures below 2000 K unless a catalyst is present. Therefore, the lack of any bond-forming or breaking reaction involving it (directly) was not surprising. For the remainder (ammonia [NH_3], hydrogen cyanide [HCN], and isocyanic acid [HNCO]), their concentrations were so low that the $|\dot{q}|$

capable of being produced by reactions involving them was also low. That, in turn, would limit those reactions' potential to impact T. Since comparative values of T and $\dot{q}$ were the basis for eliminating reactions, it is understandable that no reactions involving NH_3, HCN, or HNCO would be retained. However, it should be appreciated that this result should not be taken to imply that the levels of NH_3, HCN, and HNCO emitted by the M4 are not a function of the chemical kinetics occurring during muzzle blast. Rather, to establish any such dependence via simulations with the muzzle-blast CFD model, it will be necessary to generate (new) reduced mechanisms employing screening protocols that monitor the concentrations predicted for them by trial mechanisms and compare them to those predicted by the full mechanism.

The inclusion of reactions involving the creation of CH_3 (radicals) from methane [CH_4] caught our attention because we could envision them seeding the creation of molecules containing more than one C atom. However, the only such molecule not eliminated by the screening protocol (at the maximum MADs) was CH_3OCO.

It was observed that the only significant changes in species' X_k occurred during the first microsecond of the simulations. Figure 4 shows results from the SM(27R-22S)-based VTIM simulation for the five species with the largest X_k (CO, H_2O, CO_2, N_2, and H_2). Combined, their X_k summed to greater than 0.99 at t_0. All but N_2 were reactive, but their X_k did not vary much. Given that the relative concentrations of these species were specified to be in a state that was close to equilibrium at t_0, and only a small amount of O_2 was added to the system, this finding was not particularly surprising. The perturbations in X_{H2O} and X_{H2} were slightly larger than those in X_{CO2} and X_{CO}. Foreshadowed by the large fraction of the mechanisms' reactions that involved species whose only elements were H and/or O, these findings also suggest that radicals created by the O_2-induced oxidation of H_2 will be influential in muzzle-blast chemical kinetics.

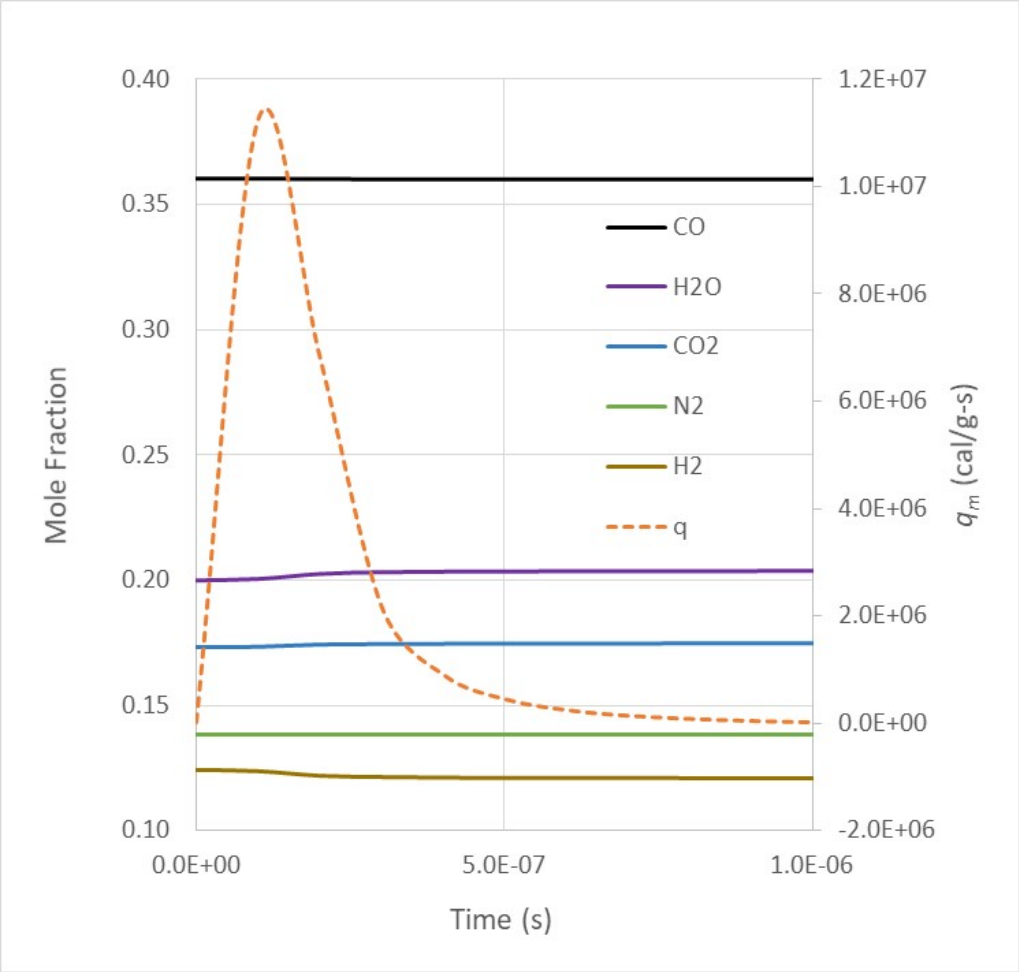

Fig. 4 Heat-release rate and mole fractions of major species as a function of time: SM(27R-22S)-based VTIM simulation

Figure 5 shows the changes with t in the X_k of the other three reactive species present at t_0 (O_2, CH_4, and H) as well as intermediate products whose X_k at some point reached a value greater than 2×10^{-7}. (That threshold excluded CH_3O and CH_3OCO, whose X_k never exceeded 2×10^{-9}.) As shown, the added O_2 was rapidly consumed. X_{CH4} remained relatively constant, while X_H increased significantly before being consumed. Of the newly created species' X_k, only HO_2's ever exceeded 1×10^{-4} (0.01%).

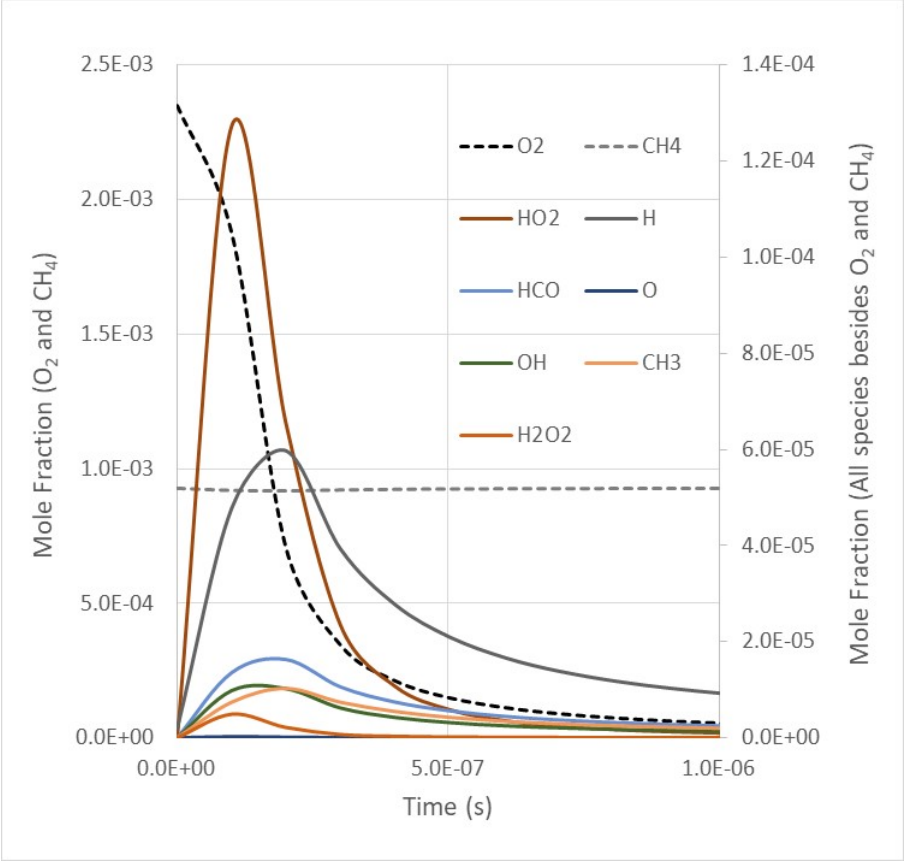

Fig. 5 Mole fractions of minor species as a function of time: SM(27R-22S)-based VTIM simulation

4. Recommendations for Analyzing Muzzle-Blast Simulations

As discussed in Section 2.1, an OFDF-based screening protocol might be better for producing skeletal mechanisms for muzzle-blast CFD models than an HR-based one. However, we lacked sufficient knowledge of the conditions in the flow field to justify formulating and implementing one. Looking forward to the analysis of muzzle-blast simulations, we note that concentration mappings of some of the species in SM(22R-20S) or SM(27R-22S) would likely be helpful in addressing this issue. Shown in Table 3, they fall into three classes: 1) a nonreactive species found only in air (Ar), 2) end products of the (non-O_2 supplemented) combustion of the propellant that are not afforded an opportunity to react by either SM(22R-20S) or SM(27R-22S) (NH_3, HCN, HOCHO, and/or HNCO), and 3) species whose production will be enhanced by the mixing of the muzzle effluent with air (HO_2, H, HCO, O, OH, and H_2O_2). Having the potential to pinpoint critical regions of mixing and reactivity, they would identify the conditions required for significant reactivity to occur, and thereby provide guidance for the formulation of relevant OFDF problems (not to mention more-representative HR problems).

Table 3 Species whose concentrations mappings would be instructive for formulating HR and OFDF simulations for future TMM screening protocols

Nonreactive; air only	Nonreactive; non-O_2 supplemented propellant combustion product only	Reactive; mixing layer enhanced	Nonreactive; bullet shot line
Ar	NH_3	HO_2	N_2*[a]
	HCN	H	
	HOCHO	HCO	
	HNCO	O	
		OH	
		H_2O_2	

[a] Surrogate for N_2.

In addition, we are also curious as to whether the air that is compressed ahead of the bullet plays a greater role than the air outside that path in furthering the oxidation of the muzzle effluent. To investigate this issue, we suggest specifying a "species"/surrogate with attributes identical to N_2 (say N_2*), and substituting it for N_2 in the air in the path of the bullet. Since N_2 is not directly involved in any reaction in SM(22R-20S) or SM(27R-22S), no modifications to these mechanisms' reaction sets would be required. N_2*'s presence behind the bullet would be solely due to molecular transport, and as such, mappings of its concentration would indicate where air in the path of the bullet ends up. Compared with mappings of the temperature field and reaction intermediate concentrations, correspondences between them would indicate a reactivity enhancing effect.

5. Summary and Conclusions

The TMM was employed to generate baseline chemical kinetics mechanisms for modeling M4 muzzle blast. Targeting simulations in which it will be assumed that the combustion of the NC-NG-based propelling charge is complete prior to the bullet exiting the muzzle, the formulation of the screening protocol involved performing thermochemical equilibrium calculations to estimate the T, P, and $\{X_k\}$ of the gas in an M4's barrel at the moment the bullet exits. A nominal case was translated into initial conditions for HR simulations, and they were modified to include an amount of air that might be expected to mix with the effluent during the first millisecond following the bullet's exit. Based on a CONP problem, the screening protocol was applied to a mechanism comprising 2751 elementary reactions and 813 species deemed likely to well represent the chemical kinetics attending the muzzle effluent's expansion and mixing with air. It was found that skeletal mechanisms with as few as 22 reactions and 20 species produced values for critical parameters of the solution that well reproduced those produced with the

full mechanism. In addition, values for critical parameters of the solutions the skeletal mechanisms produced for a VTIM problem that was considered a better approximation of an actual blast were also in good agreement with those produced with the full mechanism.

Based on the evaluations performed, two candidates were recommended for use in the muzzle-blast CFD model: one with 22 reactions and 20 species, and one with 27 reactions and 22 species. All the inputs needed to construct them are provided in an addendum to this report (McQuaid et al. 2021). For convenience, parameter sets for computing the species' molecular transport properties are also provided therein. Recommendations for analyzing muzzle-blast simulations based on these mechanisms were also suggested. In particular, species whose concentration mappings would pinpoint critical regions of mixing and reactivity were identified.

6. References

Anderson WR, Meagher NE, Vanderhoff JA. Dark zones of solid propellant flames: critical assessment and quantitative modeling of experimental datasets with analysis of chemical pathways and sensitivities. Army Research Laboratory (US); 2011a. Report No.: ARL-TR-5424.

Anderson WR, Meagher NE, Vanderhoff JA. Dark zones of solid propellant flames: critically assessed datasets, quantitative model comparison, and detailed chemical analysis. Combust Flame. 2011b;158:1228–1244.

Bastea S. Cheetah 9.0. Lawrence Livermore National Laboratory; 2019.

Benson SW. Thermochemical kinetics. New York (NY): John Wiley and Sons; 1976.

Caracotsios M, Stewart WE. Sensitivity analysis of initial value problems with mixed ODEs and algebraic equations. Comp Chem Eng. 1985;9(4):359–365.

Chen CC, Anderson WR, McQuaid MJ. Computationally based predictions for the burning rates and flame structures of nitroglycerin doped with various small molecules. Army Research Laboratory (US): 2019 June. Report No.: ARL-TR-8721.

Chen CC, McQuaid MJ. Thermochemical and kinetic studies of the pyrolysis of hydroxyl-terminated polybutadiene (HTPB). Presented at the 43rd JANNAF Combustion Subcommittee Meeting; 2009 Dec 7–11; La Jolla, CA.

Chen CC, McQuaid MJ. Thermochemistry and kinetics modeling of hydroxyl-terminated polybutadiene-red fuming nitric acid (HTPB-RFNA) systems. Presented at the 5th JANNAF Liquid Propulsion Subcommittee Meeting; 2010 May 3–7; Colorado Springs, CO.

Chen CC, McQuaid MJ. Thermochemistry and kinetics modeling of the oxidation of hydroxyl-terminated polybutadiene in air. Presented at the 44th JANNAF Combustion Subcommittee Meeting, 2011 Apr 18–22; Arlington, VA.

Chen CC, McQuaid MJ. Thermochemical and kinetics modeling pertaining to AP-HTPB composite propellant combustion. Presented at the 39th JANNAF Propellant and Explosives Development and Characterization Meeting; 2015 Dec 7–10; Salt Lake City, UT.

Chen CC, McQuaid MJ. A skeletal, gas-phase, finite-rate, chemical kinetics mechanism for modeling the deflagration of ammonium perchlorate-hydroxyl-terminated polybutadiene composite propellants. Army Research Laboratory (US); 2016 Apr. Report No.: ARL-TR-7655.

Chen CC, McQuaid MJ. A skeletal finite-rate chemical kinetics mechanism for modeling HTPB-air combustion in a gun-launched solid-fuel ramjet combustor. DEVCOM Army Research Laboratory (US); 2020 Jan. Report No.: ARL-TR-8891.

Horst AW. A brief journey through the history of gun propulsion. Army Research Laboratory (US); 2005 Nov. Report No.: ARL-TR-3671.

Kee RJ, Rupley FM, Miller JA, Coltrin ME, Grcar JF, Meeks E, Moffat HK, Lutz AE, Dixon-Lewis G, Smooke MD, et al. CHEMKIN collection, rel. 3.7. Reaction Design, Inc; 2002.

Kotlar AJ. A general approach for the reduction of chemical reaction mechanisms. I: methodology and application to MMH-RFNA. Presented at the 5th JANNAF Liquid Propulsion Subcommittee Meeting; 2010 May 3–7; Colorado Springs, CO.

Li S, Petzold LR. Design of new DASPK for sensitivity analysis. Department of Computer Science, University of California; 1999. Report No.: TRC99-28.

Lutz, AE, Kee RJ, Miller JA. SENKIN: a Fortran program for predicting homogeneous gas phase chemical kinetics with sensitivity analysis. Sandia National Laboratories; 1988. Report No.: SAND96-8248.

Lutz, AE, Kee RJ, Grcar JF, Rupley FM. OPPDIF: a Fortran program for computing opposed-flow diffusion flames. Sandia National Laboratories; 1997. Report No.: SAND96-8243.

Mayer J, Hart B. Simplified equations of interior ballistics. Journal of the Franklin Institute 1945; 240,401–411.

McNesby K, Nusca M, McQuaid M, Chen CC, Benjamin R, Thompson R, Sickels W, Summers G, Sparks R, Gullett B, et al. Development of methodologies for evaluating emission from metal-containing explosives and propellants. In: SERDP SEED project (WP-2611) – final report. Strategic Environmental Research and Development Program; 2018.

McQuaid MJ. The trial mechanism method for chemical kinetics mechanism reduction: an approach to developing mechanisms with wider ranges of applicability. Presented at the 7th JANNAF Liquid Propulsion Subcommittee Meeting; 2013a Apr 29–May 2; Colorado Springs, CO.

McQuaid MJ. Chemical kinetics mechanism reduction based on principal component analysis: development and testing of some new implementations. Army Research Laboratory (US); 2013b May. Report No.: ARL-TR-6449.

McQuaid MJ. An opposed-flow diffusion flame simulation-based implementation of the trial mechanism method for chemical kinetics mechanism reduction: application to the San Diego mechanism for HTPB-air combustion modeling. DEVCOM Army Research Laboratory (US); 2020 Aug. Report No.: ARL-TR-9032.

McQuaid MJ, Chen CC, McNesby K, Schmidt J. Addendum to ARL-TR-9155, predicting M4 carbine pollutant emissions: baseline skeletal finite-rate chemical kinetics mechanisms for muzzle blast modeling. DEVCOM Army Research Laboratory; 2021 Feb. Report No.: ARL-TN-1048.

Stone CP. Summary of user productivity enhancement, technology transfer, and training (PETTT) refactoring assistance for chemical kinetics analysis tools at CCDC Army Research Laboratory (US); 2020 Jan. Report No.: ARL-CR-0843.

Zhang H, Chen Z, Jiang X, Li H. Investigations on the exterior flow field and efficiency of the muzzle. Journal and Mechanical Science and Technology 2013;27:95–101.

List of Symbols, Abbreviations, and Acronyms

1-D	one-dimensional
Ar	argon (atom)
ATOL	absolute tolerance
C	carbon (atom)
CFD	computational fluid dynamics
CH_4	methane
CO	carbon monoxide
CO_2	carbon dioxide
CONP	constant pressure (problem)
eq	equilibrium
H_2	hydrogen
H_2O	water
H_2O_2	hydrogen peroxide
HCN	hydrogen cyanide
HCNO	isocyanic acid
HR	homogeneous reactor
HTPB	hydroxyl-terminated polybutadiene
k	species
MADs	maximum acceptable deviations
N_2	nitrogen
NATO	North Atlantic Treaty Organization
NC	nitrocellulose
NG	nitroglycerine
NH_3	ammonia
O_2	oxygen
OFDF	opposed-flow diffusion flame

ρ	density
P	pressure
$\dot{q}$	heat release rate
R	universal gas constant
RFNA	red fuming nitric acid
RTOL	relative tolerance (parameter)
t	time
T	temperature
T_f	final temperature
TMM	trial mechanism method
V	(effluent/mixture) volume
V_0	initial volume
VTIM	volume expansion versus time (problem)
W_k	molecular weight of the k^{th} species
X_k	mole fraction of the k^{th} species
Y_k	mass fraction of the k^{th} species

1 (PDF)	DEFENSE TECHNICAL INFORMATION CTR DTIC OCA
1 (PDF)	DEVCOM ARL FCDD RLD DCI TECH LIB
3 (PDF)	ENVIROMENTAL PROTECTION AGENCY B GULLETT A HOLDER I GILMOUR
2 (PDF)	STRATEGIC ENVIRONMENTAL RESEARCH AND DEVELOPMENT PROGRAM R NISSAN B LEWIS
1 (PDF)	UDRI – UNIVERSITY OF DAYTON RESEARCH INSTITUTE J AURELL
10 (PDF) 5 (HC)	DEVCOM ARL FCDD RLW WA K MCNESBY FCDD RLW WC M MCQUAID (5 HC) C-C CHEN J SCHMIDT M NUSCA A WILLIAMS D GUBERNAT J VEALS A MCBAIN M MINNICINO